Chinese Journal of Polar Science, Vol. 10, No. 1, 51 - 60, June 1999

The relationship between polar sea ice and the precipitation and temperature over China revealed by using SVD method

Liu Jiping (刘骥平) and Bian Lingen (卞林根)

Chinese Academy of Meteorological Sciences, Beijing 100081, China

Received October 13, 1998

Abstract The relationship between polar sea ice anomalies and the precipitation and temperature anomalies over China is investigated by performing singular value decomposition (SVD) analyses. The first three coupling modes have been studied. Analyses show that there exist key areas of polar sea ice which are highly related with the precipitation and temperature anomalies over China. Different spatial anomaly patterns of these areas of polar sea ice are followed by different spatial anomaly patterns of the precipitation and temperature over China.

Key words Arctic and Antarctic sea ice, precipitation, temperature, SVD.

1 Introduction

Recently, whether polar is the most sensitive region to global climate change greatly concerns many scholars. The change of polar sea ice is of particular interest because of its special feedback mechanisms in atmosphere-ocean-ice interaction (Gloersen *et al.* 1992). Spatial and temporal variation of polar sea ice determines an important contribution to the advective heat and salt exchange between the polar region and the rest of the globe (Walsh 1983). Lots of studies have shown that the variation of polar sea ice is an indicator of climate change (Walsh and Jhonson 1979a; Bian *et al.* 1997). But the relationships between polar sea ice and other meteorological elements have been studied inadequately. Especially when studying the effect of the variation of polar sea ice on atmospheric circulation and climate, different scholars have divided polar sea ice into different sectors according to different standards (Simmonds 1995; Walsh and Jhonson 1979b). Therefore their conclusions have great differences. The SVD method provides an objective technique to better deal with this issue. Based on the analysis of annual and seasonal variation of polar sea ice, the relationship between polar sea ice and the precipitation and temperature over China has been studied in this paper by using SVD method.

2 SVD method and data source

(1) The SVD (singular value decomposition) method (Zhang 1994; Wallace *et al.* 1992) is based on the maximum covariance between two different fields so that it could

find in what mode the relation of two different fields reaches the maximum. It uses a few eigenvectors to explain major covariance of two different fields. Therefore, the SVD method is a useful tool to study the relationship of two different fields. Assuming that X_{nt} and Y_{mt} denote two different fields, where the subscripts n and m represent space and subscript t represents time (where n is not equal to m).

The covariance matrix of two different fields is $Z_{nm}=X_{nt}Y'_{mt}$.

Using singular value decomposition, Z_{nm} can be rewritten as $Z_{nm}=\sum_{i=1}^{k}\sigma_i U_i V'_i$.

Where orthogonal function of U_i and V_i are the left and right singular vectors respectively. σ_i is singular value and $\sigma_1 \geqslant \sigma_2 \geqslant \Lambda \geqslant \sigma_k \geqslant 0$. Percentage covariance of the ith coupling mode of two fields in total covariance is as following: $P=\frac{\sigma_i^2}{\sum_{i=1}^{k}\sigma_i^2}$

(2) The sea ice data were obtained from NSIDC. Arctic sea ice data are for a period of 94 a (1901 - 1994) and Antarctic sea ice data are for a period of 18 a (1973 - 1990). The 80×58 rectangular grids overlay the North Polar region and 80×80 rectangular grids overlay the South Polar region with equal area projection. Temperature and precipitation data used in this paper are data of 160 stations of China. We computed the average of Jun. - Jul. - Aug. and Dec. - Jan. - Feb. standing for summer and winter.

3 Characteristics of annual and seasonal variation of polar sea ice

Fig. 1 (a, b, c) shows annual and seasonal variation of the area of polar sea ice. The area of Arctic sea ice reached its maximum during the ending of the 1940's and the beginning of the 1950's and its sub-maximum are at the ending of the 1910's, the middle period of the 1930's and the ending of the 1960's. Worthy of mention is that the area of Arctic sea ice decreased continuously from the beginning of the 1970's to now. There are two sudden decreases at the beginning and the ending of the 1970's. The area of Antarctic sea ice exhibits obvious quasi-three years oscillation, but no obvious decreasing trend as that of Arctic sea ice.

The area of Arctic sea ice reaches its maximum at February and minimum at August and that of Antarctic sea ice reaches its maximum at September and minimum at February. The amplitude of seasonal variation of Antarctic sea ice is much larger than that of Arctic sea ice, which might be caused by great different geographical condition of the two polar regions.

4 The relationship between polar sea ice and temperature and precipitation over China

Based on the analyses of seasonal variation of the area of polar sea ice, we defined the difference of sea ice area between August and February of the following year and between February and August of the same year standing for variation of freezing and melting periods of Arctic sea ice. And the difference between September and February of the following year and between February and September of the same year as variation of melting and condensation periods of Antarctic sea ice. Then SVD method is applied to

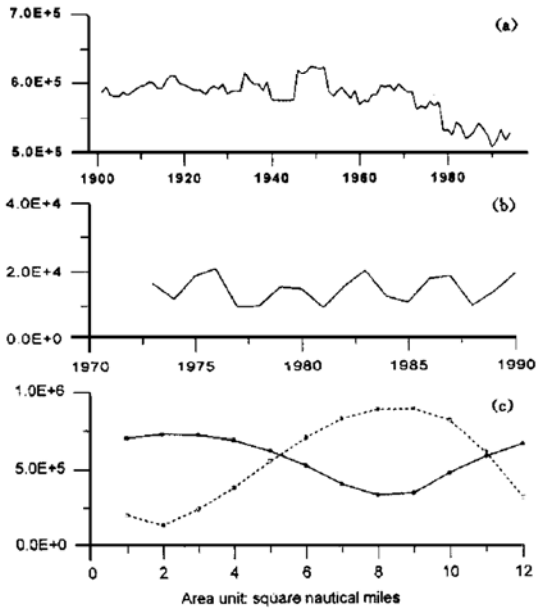

Fig. 1. (a) Annual variation of Arctic sea ice; (b) Annual variation of Antarctic sea ice; (c) Seasonal variation of polar sea ice (Arctic: solid line; Antarctic: dash line).

variation of rainfall — than that of temperature. study the relationship between the variation of freezing and melting periods of polar sea ice and precipitation and temperature over China.

Here (Table 1), the first three modes for the variation of freezing and melting periods of Arctic and Antarctic sea ice and the following summer and winter temperature explain 74%, 64% and 84%, 82% of total covariance. Worthy of note is that the variation of melting period of polar sea ice has higher correlation with the following summer and winter temperature than that of the freezing period. For the following summer and winter rainfall, the first three modes only explain 47%, 52% and 46%, 50% of total covariance, which may be caused by more complicated spatial and temporal

Table 1. Percentage of variance explained by the first three coupling modes

Period	Aug. —Feb. (N)		Feb. —Aug. (N)		Sep. —Feb. (S)		Feb. —Sep. (S)	
	Temp	Rain	Temp	Rain	Temp	Rain	Temp	Rain
1	0.43	0.26	0.59	0.29	0.36	0.17	0.58	0.23
2	0.23	0.13	0.19	0.13	0.19	0.17	0.15	0.15
3	0.08	0.08	0.06	0.10	0.09	0.12	0.09	0.12
Sum	0.74	0.47	0.84	0.52	0.64	0.46	0.82	0.50

4.1 Relationship between Arctic sea ice and the temperature and precipitation over China

The first three coupling modes for variation of freezing period of Arctic sea ice area and the following summer temperature anomaly are shown in Fig. 2. In the first mode, negative sea ice anomalies in Bering strait and north part of the Bering Sea, Beloje More, around the Hudson Bay and positive anomalies in west part of the Baffin Bay are associated with strong negative temperature anomalies between the Yellow River and the Yangtze River, Qinhai and Gansu province. In the second mode, positive sea ice anomalies in east part of the Hudson Bay and the Hudson Strait are associated with negative temperature anomaly throughout eastern China. In the third mode, positive sea ice anomalies in the Chukchi Sea, north part of the Baffin Bay and west part of the Kara Sea are associated with positive temperature anomaly in the Huabei plain.

Fig. 3 Shows the first three modes for variation of melting period of Arctic sea ice area and the following winter temperature anomaly. The first mode explains 59% of total covariance. Negative sea ice anomalies in the Bering Strait and north part of the Bering

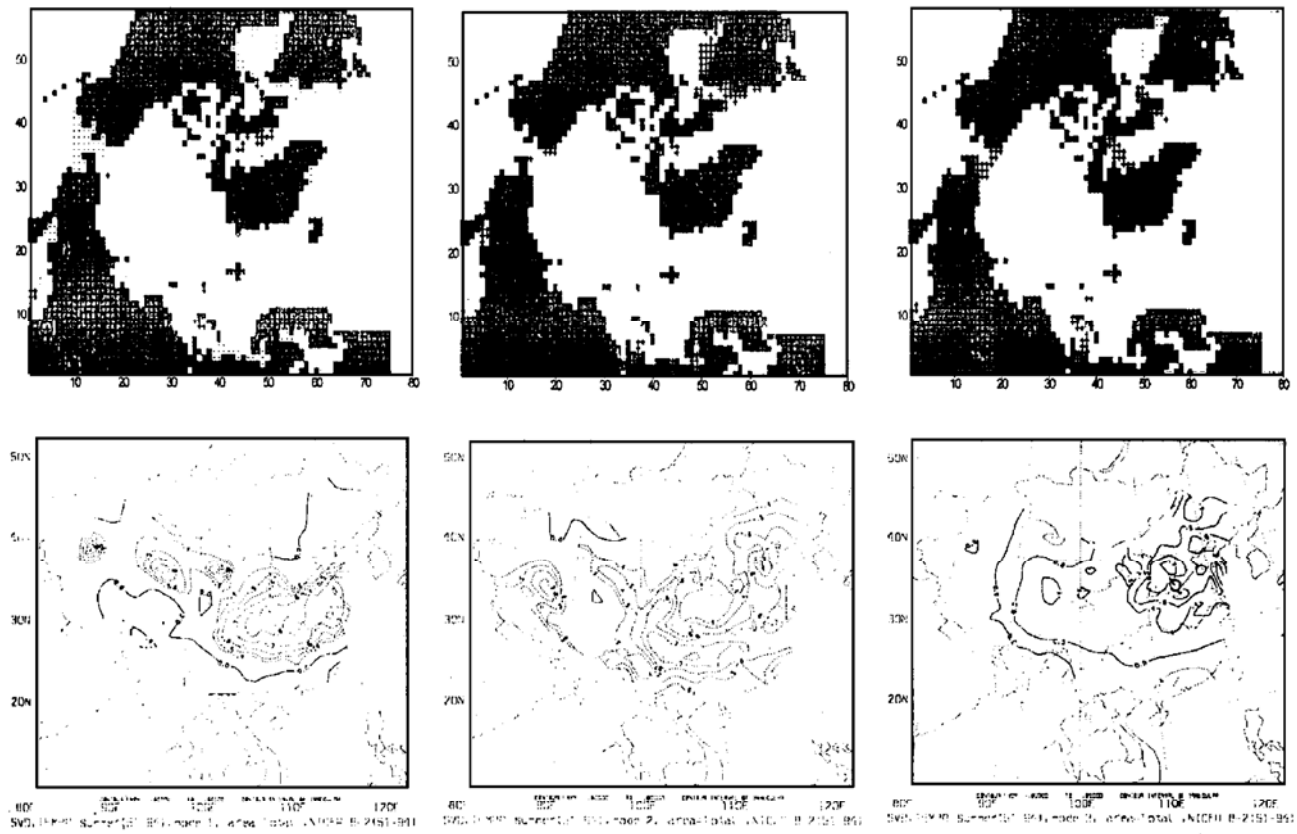

Fig. 2. The first three modes for freezing period of Arctic sea ice and the following summer temperature.

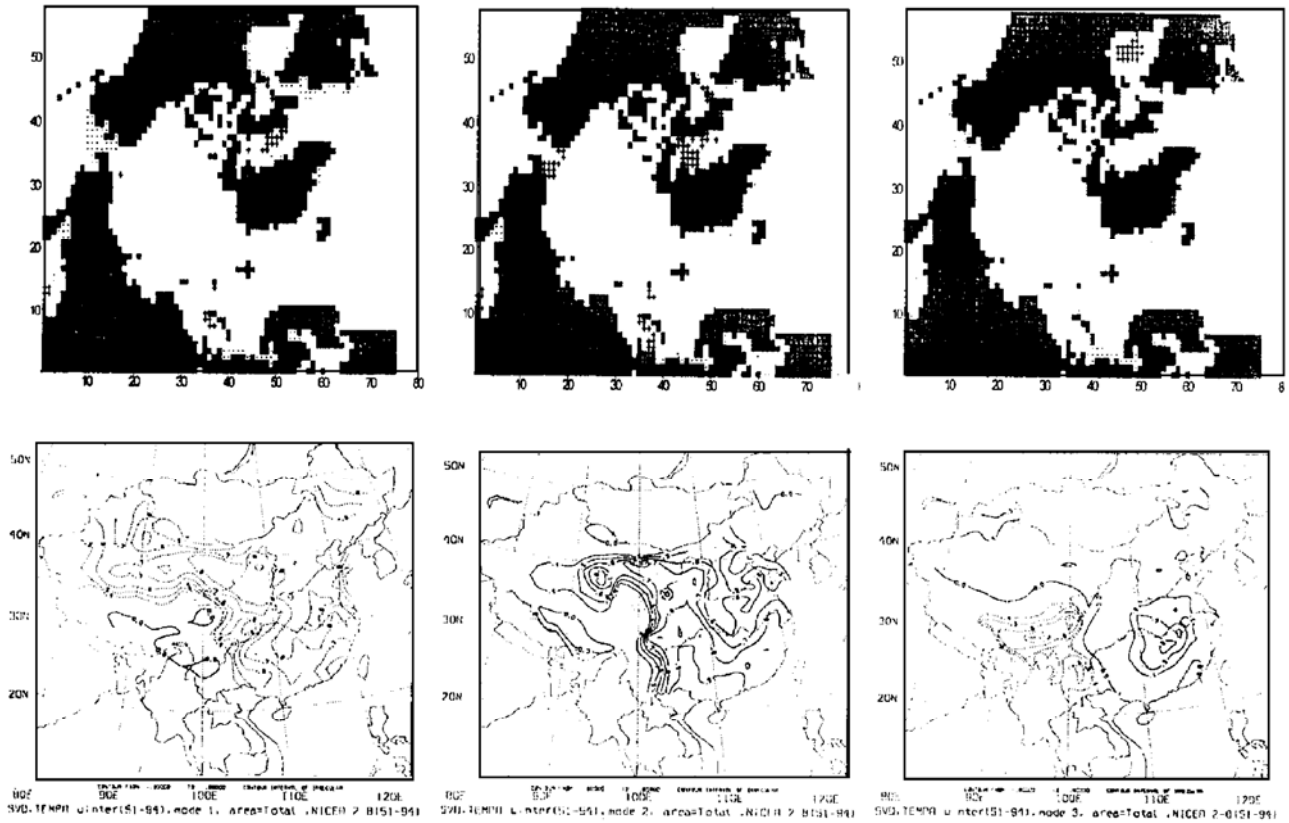

Fig. 3. The first three modes for melting period of Arctic sea ice and the following winter temperature.

Sea, Hudson Strait, Beloje More and positive sea ice anomaly in west part of the Baffin Bay are associated with negative temperature anomalies throughout whole China, especially eastern China. For the second mode, positive sea ice anomalies in the Chukchi Sea, the Baffin Bay, the Kara Sea are associated with strong positive temperature anomalies in Qinhai province and southeast China. For the third mode, positive sea ice anomaly in mid-part of the Hudson Bay and negative sea ice anomaly in Beloje More are associated with positive temperature anomaly in mid-stream of the Yangtze River and negative temperature anomaly in southwest China.

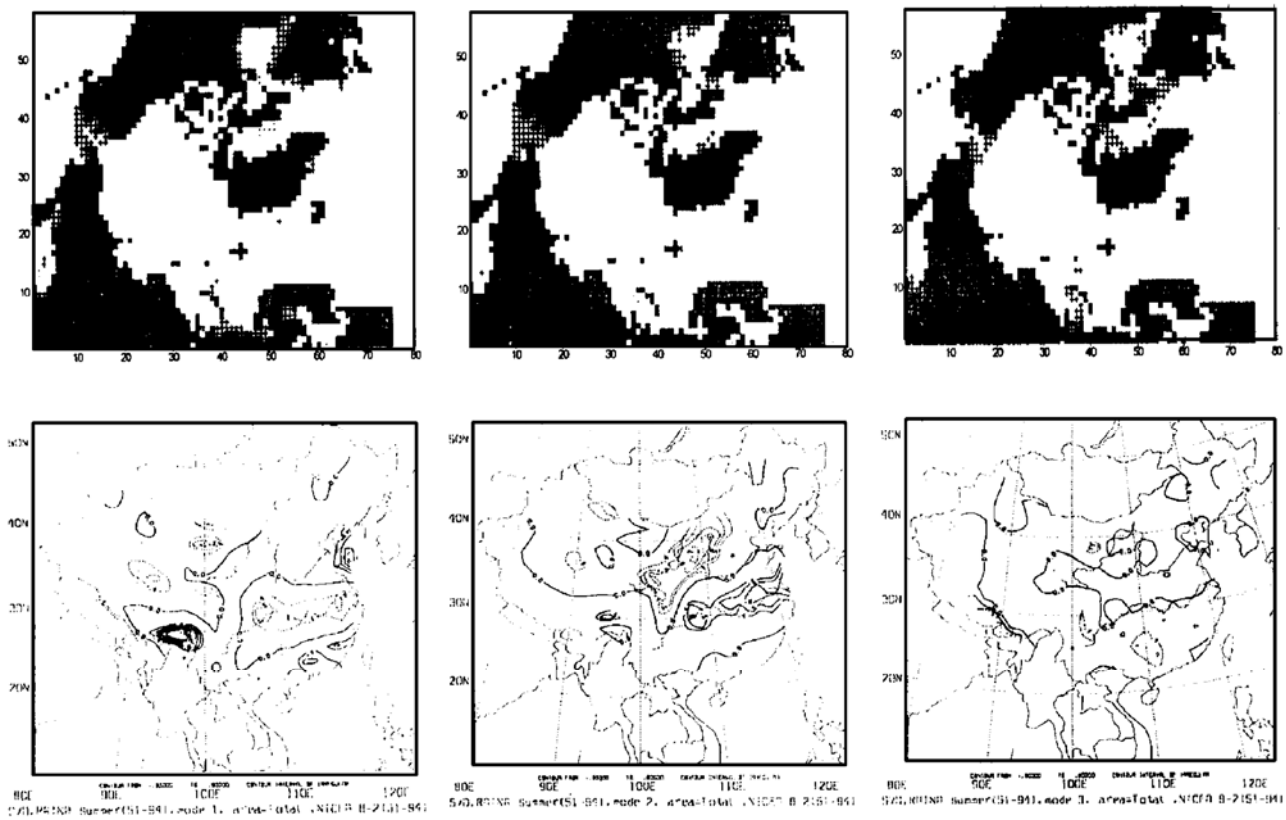

Fig. 4. The first three modes for condensation period of Arctic sea ice and the following summer rainfall.

Fig. 4 shows the first three modes for variation of freezing period of Arctic sea ice area and the following summer rainfall anomaly. In the first mode, strong positive sea ice anomalies in the Bering Strait and north part of the Bering Sea, around the Hudson Bay, Beloje More are associated with negative rainfall anomaly in the Yangtze River and positive rainfall anomaly in the Hengduan Mountain. In the second mode, positive sea ice anomalies in the Bering Strait and north part of the Bering Sea, west part of the Hudson Bay are associated with negative rainfall anomaly in mid-stream of the Yellow River and positive rainfall anomaly in the Yangtze River. In the third mode, positive sea ice anomalies in the Chukchi Sea, the Hudson Strait and north part of the Baffin Bay and the Kara Sea are associated with weak negative rainfall anomaly on south part of China.

Fig. 5 shows the first three modes for variation of melting period of Arctic sea ice area and the following winter rainfall anomaly. In the first mode, positive sea ice anomalies in the Bering Strait and north part of Bering sea, Beloje More are associated with positive rainfall anomaly throughout whole China, especially east part of China and Chaidamu Basin. In the second mode, positive sea ice anomalies in east part of the

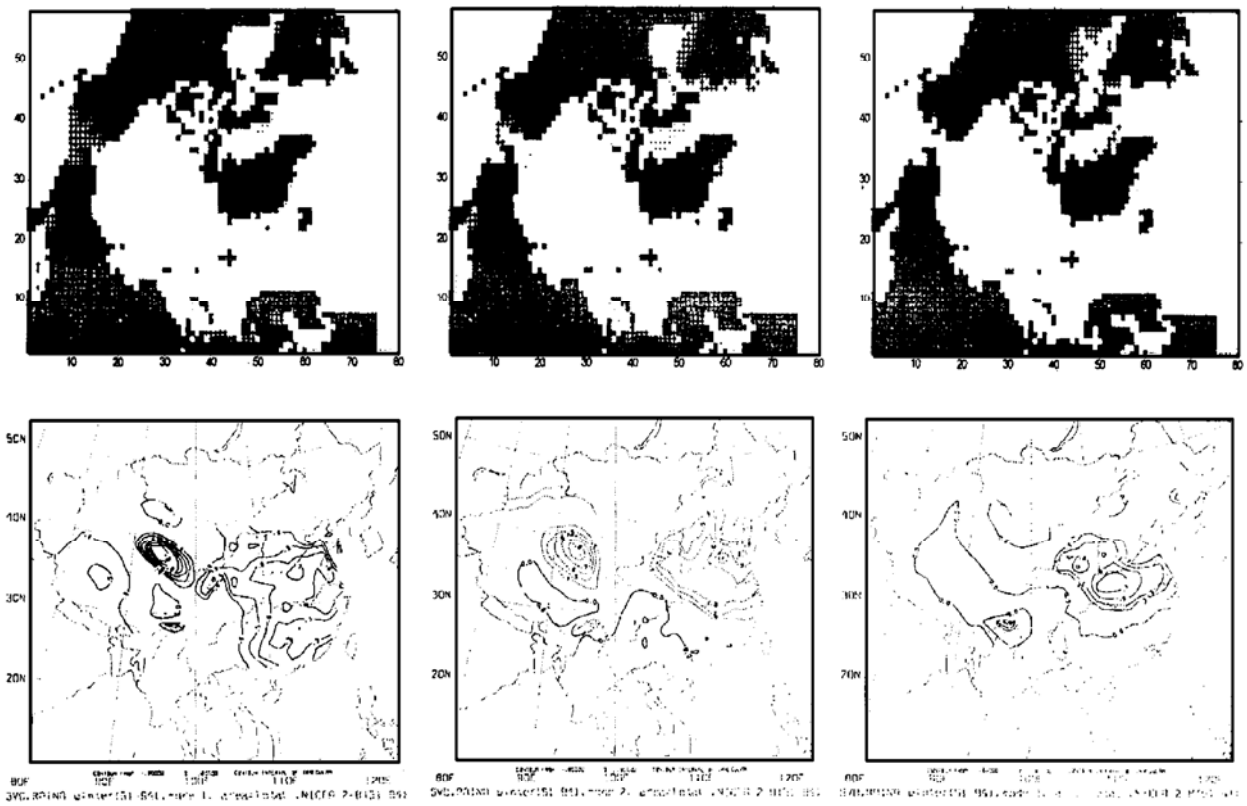

Fig. 5. The first three modes for melting period of Arctic sea ice and the following winter rainfall.

Hudson Bay and the Hudson Strait, Beloje More and negative sea ice anomaly in west part of the Baffin Bay are associated with negative rainfall anomalies between the Yellow River and the Yangtze River, the Chaidamu Basin. In the third mode, positive sea ice anomaly in west part of the Hudson Bay and the Davis Strait are associated with positive rainfall anomaly between the Yellow River and the Yangtze River.

From above discussions, key areas (above 1% significant level) of variation of freezing and melting periods of Arctic sea ice area which have high correlation with the following summer and winter temperature and rainfall anomalies over China are discovered by SVD method. They are the Bering Strait and north part of the Bering Sea, Beloje More, the Hudson Bay and Strait, the Chukchi Sea, the Baffin Bay, the Kara Sea. Different spatial anomaly patterns of these areas have accordingly different spatial anomaly patterns of temperature and precipitation over China.

4.2 Relationship between Antarctic sea ice and the temperature and precipitation over China

The first three modes for variation of freezing period of Antarctic sea ice area and the following summer temperature anomaly are shown in Fig. 6. In the first mode, negative sea ice anomalies in west part of the Ross Sea and northeast part of the Weddell Sea are associated with positive temperature anomaly throughout whole China especially east part of China and northwest part of Tibet, China. In the second mode, positive sea ice anomalies in north part of the Ross Sea and the Weddell Sea, the Davis Sea and negative sea ice anomalies in northeast part of the Weddell Sea, southwest part of the

Ross Sea are associated with negative temperature anomaly in the Yangtze River and positive temperature anomaly in southwest part of China. In the third mode, negative sea ice anomalies in north part of the Weddell Sea and the Ross Sea, the coast of the Wilkes Land are associated with positive temperature anomaly in north part of China.

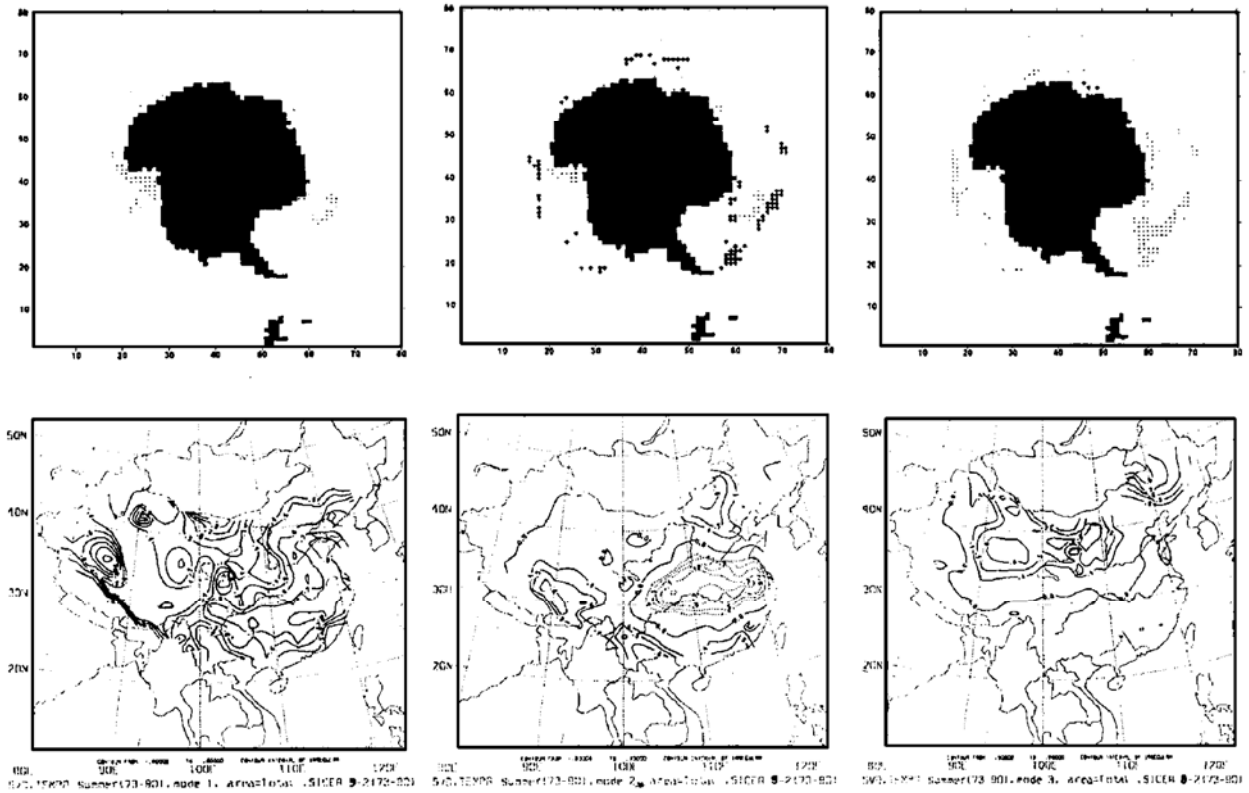

Fig. 6. The first three modes for condensation period of Antarctic sea ice and the following summer temperature.

Fig. 7 shows the first three modes for variation of melting period of Antarctic sea ice area and the following winter temperature anomaly. The first mode explains 58% of total covariance, negative sea ice anomalies in north side of the Weddell Sea and the Ross Sea and positive sea ice anomaly in the coast of the Wilkes Land are associated with strong negative temperature anomaly in eastern China. For the second mode, strong negative sea ice anomalies in north part of the Weddell Sea and northwest part of the Ross Sea are associated with negative temperature anomaly in Sichuan province of China and positive temperature anomaly in northeast China. For the third mode, negative sea ice anomalies in north part of the Weddell Sea and the Ross Sea are associated with strong positive temperature anomaly in Tibet of China.

Fig. 8 shows the first three modes for variation of condensation period of Antarctic sea ice area and the following summer rainfall anomaly. In the first mode, negative sea ice anomalies in north part of the Weddell Sea and the Ross Sea, the Haakon Ⅶ Sea are associated with strong negative rainfall anomaly in the Yangtze River and positive rainfall anomaly in north part of China. In the second mode, strong positive sea ice anomalies in north Weddell Sea, northwest part of the Ross Sea and the coast of East Antarctica are associated with negative rainfall anomaly in Tibet of China and positive rainfall anomaly in Yunnan province of China. In the third mode, positive sea ice anomaly in north part of

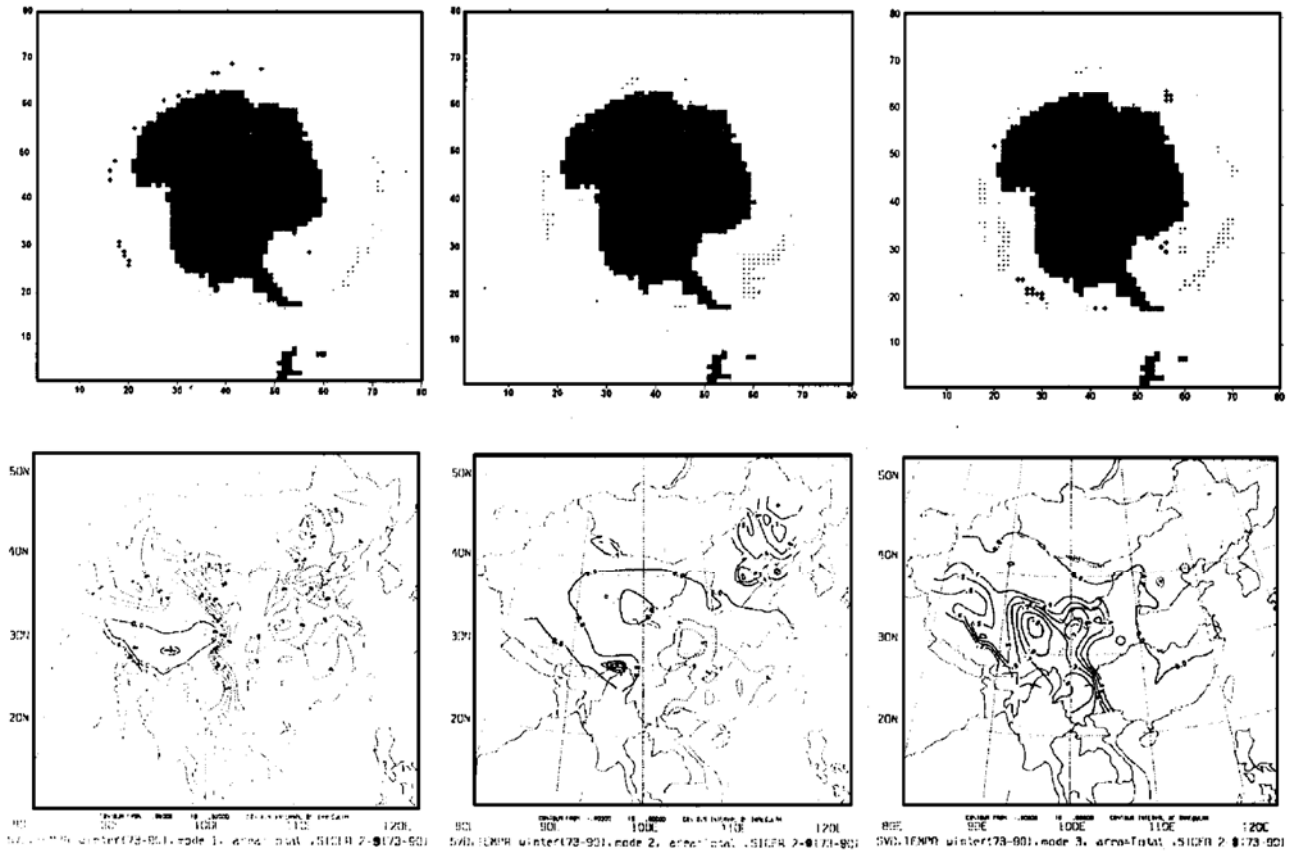

Fig. 7. The first three modes for melting period of Antarctic sea ice and the following winter temperature.

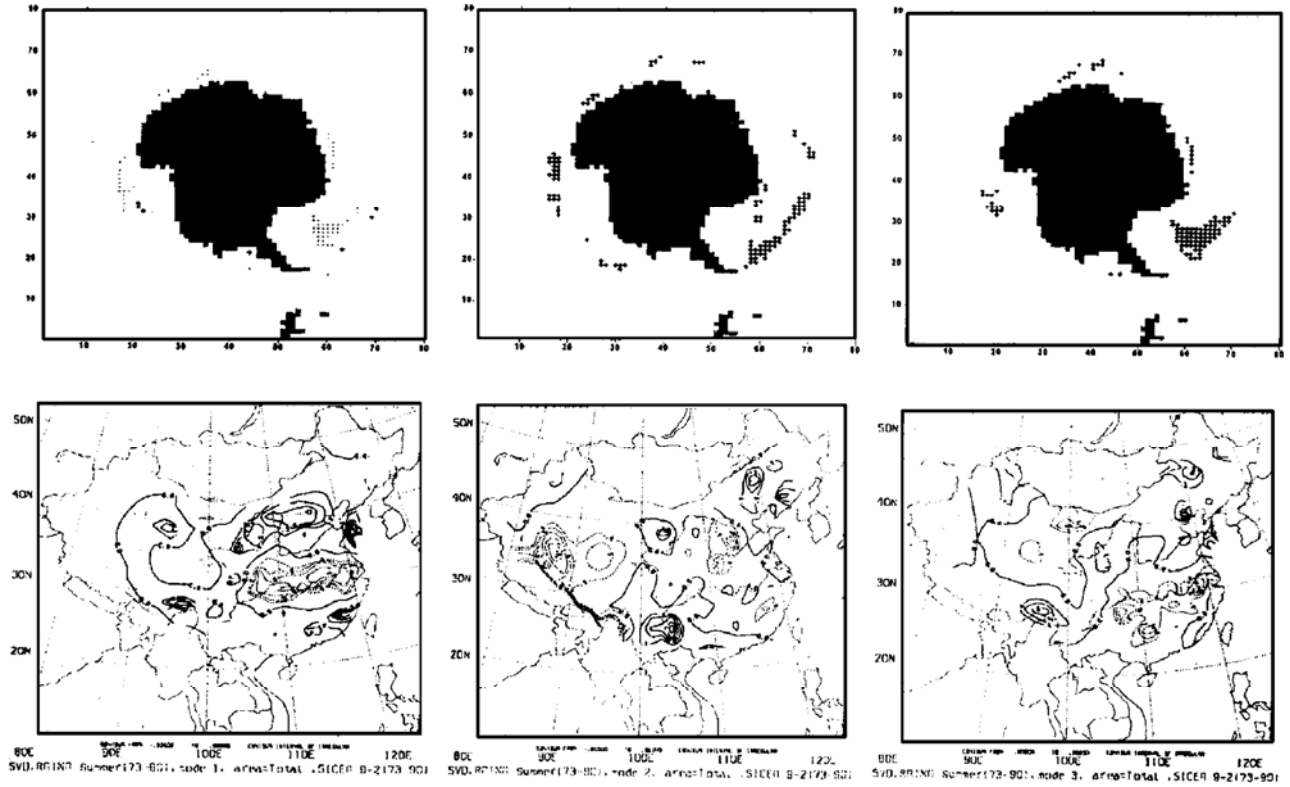

Fig. 8. The first three modes for condensation period of Antarctic sea ice and the following summer rainfall.

the Weddell Sea and the Davis Sea is associated with negative rainfall in the Yangtze River.

Fig. 9 shows the first three modes for the variation of melting period of Antarctic sea ice area and the following winter rainfall anomaly. In the first mode, negative sea ice anomaly in mid north Weddell Sea and positive sea ice anomaly in north side of the Haakon Ⅶ Sea are associated with positive rainfall anomaly throughout whole China especially eastern China and Chaidamu Basin. In the second mode, positive sea ice anomalies in whole north part of the Weddell Sea and the Ross Sea are associated with positive rainfall anomalies in mid-part of Tibet of China and Yunnan province of China. In the third mode, positive sea ice anomalies in the coast of East Antarctica, north part of the Ross Sea and negative sea ice anomalies in the south part of the Ross Sea are associated with positive rainfall anomaly in southeast part of China.

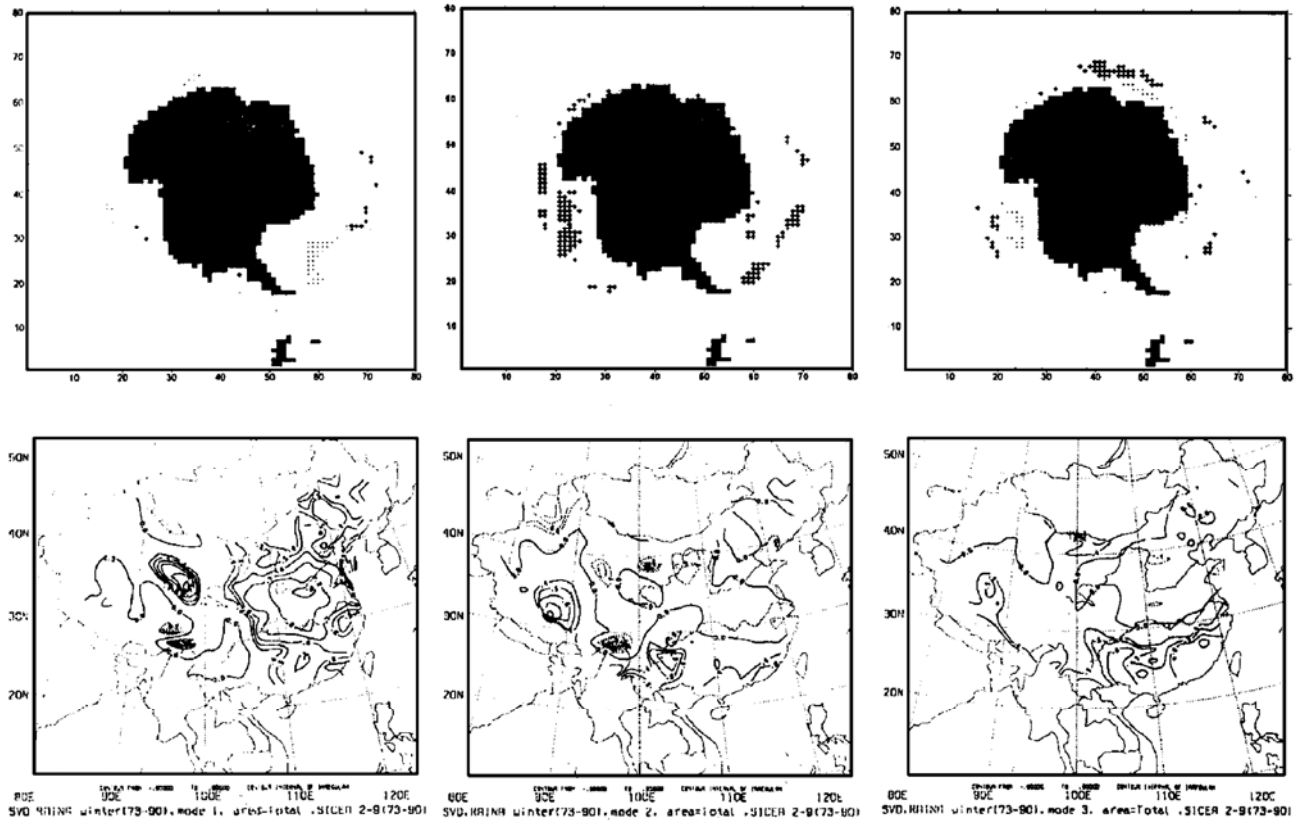

Fig. 9. The first three modes for the variation of melting period of Antarctic sea ice and the following winter rainfall.

From above discussions, key areas (above 5% significant level) of freezing and melting periods of Antarctic sea ice which have high correlation with the following summer and winter temperature and rainfall anomalies over China are the Ross Sea, the Weddell Sea, the Haakon Ⅶ Sea and the Davis Sea. Different spatial anomaly patterns of these key areas are followed by different spatial anomaly patterns of temperature and rainfall over China.

5 Conclusions

In this paper, SVD method is applied to objectively study the relationship between

polar sea ice and temperature and precipitation over China. The main results are as follows:

(1) Highly related areas between polar sea ice and temperature and precipitation are discovered by SVD method. For Arctic sea ice, key areas (above 0.01 significant level) are the Bering Strait and north part of the Bering Sea, Belije More, the Hudson Bay and Strait, the Chukchi Sea, the Baffin Bay, the Kara Sea. For Antarctic sea ice, key areas (above 0.05 significant level) are the Weddell Sea, the Ross Sea, the Haakon Ⅶ Sea, the coast of Wilkes Land, the Davis Sea.

(2) The variation of melting period of polar sea ice has higher correlation with the following summer and winter temperature than that of the freezing period. The first coupling mode explains more than half of total covariance.

(3) Different spatial anomaly modes of above key areas of polar sea ice area during variation of freezing and melting periods are followed by different spatial anomaly modes of the following summer and winter temperature and precipitation over China.

(4) The analyzed coupling modes may offer a potential clue for forecasting the trend of temperature and precipitation anomalies over China.

Acknowledgement This work was supported by the National Antarctic key project of China.

References

Bian LG, Lu LH, Jia PQ(1997): Characteristics of Antarctic surface air temperature and sea ice variations and their relationship. Chinese Journal of Atmospheric Sciences, 21(3):265 - 274.

Gloersen P, William JC, Donald JC *et al.* (1992): Arctic and Antarctic sea ice, 1978 - 1987: satellite passive-microwave observations and analysis. Washington DC: National Aeronautics and Space Administration(NASA SP; No. 511).

Simmonds I(1995): Relationship between the interannual variability of Antarctic sea ice and the southern oscillation. J. Climate, 8(3):637 - 646.

Walsh JE, Jhonson CM(1979a): Interannual atmospheric variability and associated fluctuation in Arctic sea ice extent. J. Geophy. Res, 84: 6915 - 6928.

Walsh JE, Jhonson CM(1979b): An analysis of Arctic sea ice fluctuation, 1953 - 1977. J. Physical Oceanography, 9(3):580 - 591.

Walsh JE(1983): The role of sea ice in climate variability. Atmosphere-Ocean, 23(3):230 - 239.

Wallace JM, Smith C, Bretherton CS(1992): SVD of wintertime sea temperature and 500 mb height anomalies. J. Climate, 5: 567 - 576.

Zhang JJ(1994): The Basis of medium and long range weather forecast. Beijing: Chinese Meteorological Press.